CO CRS STACK: A NEW STRATEGY TO SIMULATE CO SECTIONS BASED ON TRAVELTIME APPROXIMATION FOR A DIFFRACTED CENTRAL RAY

G. G. Garabito, P. Chira-Oliva, J. C. Ribeiro Cruz, and M. Costa

email: *german@ufpa.br*

keywords: *Finite-offset (FO) section, diffracted central ray, CO-CRS stacking algorithm*

ABSTRACT

Based on a hyperbolic traveltime approximation which depends on three kinematic attributes, the Common-Reflection-Surface (CRS) stacking method was developed to simulate zero-offset (ZO) sections. Also, following this new concept of seismic imaging, it was introduced a method to simulate common-offset (CO) sections from multicoverage data by using a hyperbolic paraxial traveltime approximation in the vicinity of a reflected central ray with finite-offset (FO). This last traveltime approximation depends on five kinematic attributes. In this work, based on this five-parameters-traveltime approximation, we obtain a new traveltime approximation for diffraction events, reducing the original formula to four parameters. We compare both traveltime approximations (reflection and diffraction events) with true traveltimes for a synthetic model. Based on the traveltime approximation for diffractions, we also present an algorithm to simulate CO sections from multicoverage data using global and local optimization methods.

INTRODUCTION

Various macro-velocity model independent methods have been introduced to simulate zero-offset (ZO) sections from multicoverage dataset. These methods are the Multifocusing (e.g Gelchinsky and Keydar (1999),Gelchinsky et al. (1999a), Gelchinsky et al. (1999b), Landa et al. (1999)), Polystack (e.g. De Bazelaire (1988)) and the Common-Reflection-Surface (CRS) (e.g. Müller (1999); Jäger et al. (2001), Garabito et al. (2001)). The CRS method uses the hyperbolic paraxial traveltime approximation in the vicinity of a ZO central ray. This formula depends on three parameters that are determined from multicoverage seismic data. The CRS method has provided high-resolution results when compared to conventional stacking method (NMO/DMO stack). These techniques have been used to stack P-P reflection events in 2-D prestack multicoverage data and to simulate ZO sections. To handle also converted waves in the frame of the CRS stack, the ZO CRS stack has been generalized to simulate CO sections (Zhang et al., 2001) The FO CRS stacking operator is constituted by five parameters, which have to be searched-for in a coherence-based, data-driven way (e.g. Zhang et al. (2001), Bergler et al. (2001c),Zhang et al. (2002)). The FO CRS stack has demonstrated the applicability not only P-P or S-S reflections, but also to seismic multicoverage data containing converted reflections, where the emergence angle information provided the FO CRS stack can be used to reliable separate P-P from P-S reflections. The in-line geometrical spreading factor can, for instance, be computed from these attributes, which is of help for Amplitude-versus-Offset (AVO) analysis (Bergler et al., 2001b). The FO CRS stack parameters may be used to determine in a subsequent traveltime inversion the P-wave velocity and/or S-wave velocity of a layered earth model (Bergler et al., 2001a).

Bergler et al. (2002) demonstrated on a synthetic dataset that the FO CRS stack can be an alternative prestack stacking tool in complex situations such as subsalt imaging. The FO CRS stack is able to produce interpretable CO sections where ZO simulation methods suffer from bad illumination of target reflectors

by small-offset reflections.
Chira-Oliva et al. (2003) investigated the sensibility of the FO CRS stacking operator with respect to the kinematic data-derived attributes. They analyzed the first derivative of this operator with respect to each one of the searched-for parameters and descried the behavior of the FO CRS stacking surface.
Boelsen and Mann (2004) discussed that the conventional FO CRS stacking operator can handle Ocean-Bottom-seismic (OBS) acquisition geometries by using a synthetic model. For this model, they compare the model-and data-derived wavefield attributes and show that the FO CRS stack provides accurate emergence angles and good results for the wavefront curvatures, too. They also present a new approach in order to process multi-component data and converted waves. This approach is able to distinguish between PP and PS reflections by combining operator shape and orientation with polarization information and provides stacked sections and kinematic wavefield attribute sections for both wave types.
Boelsen (2004) presented new hyperbolic traveltime approximations for the FO CRS stack to handle top-surface topography. He considered two types of topography: rugged and smooth. The formula for a rugged topography can be used to derive a stacking operator that is in principle to handle a vertical seismic profile (VSP) acquisition geometry as well as reverse VSP and cross-well seismic (e.g. Boelsen and Mann (2005b),Boelsen and Mann (2005a)). He also proposed an approach to perform redatuming of the FO CRS stacking section. He show the application of the FO CRS stack and the redatuming algorithm to a synthetic data set simulated with a smoothly curved measurement surface. The results showed a high-quality FO CRS stack section and accurately determined emergence angles.
In this work, based on Zhang et al. (2002), we present the particular case of a diffraction point for the FO CRS stacking operator which depends on four parameters and is called FO Common-Diffraction-Surface (CDS) stacking operator.
We applied these FO CRS stacking operators for classic configurations: common-shot (CS), common-receiver (CR), common-midpoint (CMP) and common-offset (CO). Based on these particular formulas, and considering a diffraction point in depth, we propose a new algorithm to simulate CO sections from multicoverage data.

THEORETICAL ASPECTS

HYPERBOLIC TRAVELTIME APPROXIMATION ASSOCIATED TO REFLECTED CENTRAL RAY

Following Bortfeld (1989), Zhang et al. (2001) developed a 2-D hyperbolic traveltime approximation for paraxial rays in the vicinity of a central ray, considering a finite-offset (FO) between sources and receivers. Therefore, we consider the situation in which a central ray starts at S, reflects at R on a reflector in subsurface, and emerges at the surface in G. The traveltime of paraxial rays that started at $\overline{S}$ and emerged at $\overline{G}$ (Figure 1) are obtained by

$$\begin{aligned} t^2(\Delta x_m, \Delta h) = & \left[t_0 + (\frac{\sin\beta_G}{v_G} + \frac{\sin\beta_S}{v_S})\, \Delta x_m + +(\frac{\sin\beta_G}{v_G} - \frac{\sin\beta_S}{v_S})\, \Delta h\right]^2 \\ & + t_0 \left[(4\,K_1 - 3\,K_3)\frac{\cos^2\beta_G}{v_G} - K_2\,\frac{\cos^2\beta_S}{v_S}\right]\, \Delta x_m^2 \\ & + t_0 \left[K_3\,\frac{\cos^2\beta_G}{v_G} - K_2\,\frac{\cos^2\beta_G}{v_S}\right]\, \Delta h^2 \\ & + 2\,t_0 \left[K_3\,\frac{\cos^2\beta_G}{v_G} + K_2\,\frac{\cos^2\beta_S}{v_S}\right]\, \Delta x_m\, \Delta h \end{aligned} \tag{1}$$

where t_0 is the traveltime along the central ray, β_S and β_G are the emergence angles of the central ray in the position of the source S and the receiver G, respectively. The dislocations $\Delta x_m = x_m - x_0$ and $\Delta h = h - h_0$ correspond to the midpoint and half-offset, respectively, where $x_0 = (x_G + x_S)/2$ is the midpoint and $h_0 = (x_G - x_S)/2$ is the half-offset of the central ray. The coordinates of the sources and receivers are denoted by x_S and x_G. The midpoint $x_m = (\overline{x}_G + \overline{x}_S)/2$ and half-offset $h = (\overline{x}_G - \overline{x}_S)/2$ are the coordinates of an arbitrary paraxial ray with finite-offset, where the coordinates of the source and receiver are denoted by $\overline{x}_S$ and $\overline{x}_G$, respectively. The wave velocity at the source S and receiver G are

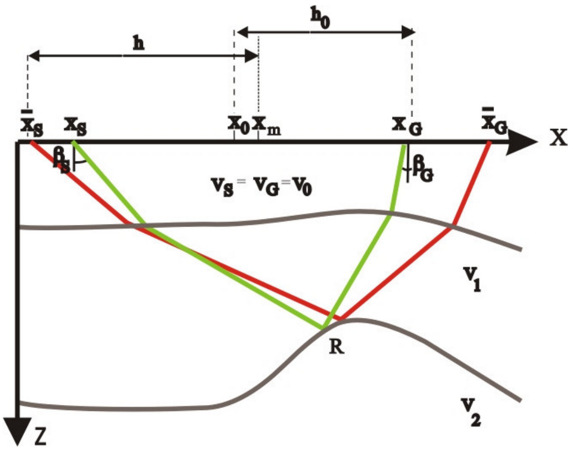

Figure 1: 2-D model of three homogeneous layers separated by curved and smooth interfaces, where x_S and x_G are the coordinates of the source and receiver of the central ray (green line), with x_0 and h_0 denoting the midpoint and half-offset coordinates of this ray. $\overline{x}_S$ and $\overline{x}_G$ denote the coordinates of the source and receiver of a paraxial ray (red line). x_m and h denote the midpoint and half-offset coordinates of this ray. The angles β_S and β_G denote the emergence angles of the central ray at the source and receiver with respect to the normal of the measurement surface.

denoted by v_S and v_G, respectively. In this work, we consider the near surface velocity $v_S = v_G$ as constant. The quantities, K_1, K_2 and K_3 are wavefront curvatures associated to the central ray (Figure 2a,b), computed at the respective emergence points. This expression (1) is called FO CRS stacking operator.

The wavefront curvatures (K_1,K_2,K_3) are associated to a real common-shot (CS) experiment and a hypothetical common-midpoint (CMP) experiment, respectively. In both experiments, the positions of the source and receiver coincide with the initial and final positions of the central ray. As shown in Figure 2a, in the CS experiment a source generates a wave in S that propagates downwards along the central ray, reflects on the second reflector, and propagates towards the surface, where it is measured at G the emerging wavefront curvature K_1 .The propagation associated with the central ray for different instants of time is depicted in Figure 2a. Figure 2b illustrates an hypothetical CMP experiment, where the propagation of the wave associated to the central ray is depicted at different instants of time. In this experiment, the wavefront starts in S with curvature K_2, propagates downwards along the central ray, reflects on the second interface and emerges at G with curvature K_3. Curvature K_2 has a negative signal according to the convention of Hubral and Krey (1980), which states when a wavefront is in front of its tangent plane, with respect to the direction of propagation.

Considering a given velocity model, curvatures K_1, K_2 and K_3, as well as the angles β_S and β_G associated to a central ray, can be calculated by forward modeling, using a ray-tracing program (Cerveny and Psensik, 1988) and applying the transmission and reflection laws of wavefronts, as shown in Hubral and Krey (1980). To represent the CRS stacking operators associated to a FO central ray, we consider a synthetic model (lower part of Figure 3) constituted of three separated by curved and smooth interfaces with velocities $v_s = v_G = v_0 = 1500 m/s$, and $v_3 = 3700 m/s$, respectively. By using the ray-tracing algorithm, the traveltimes of primary reflections for different CO (equation 1) are computed. The blue curves represent the CO traveltimes of primary reflections associated to the second reflector (Figures 3 and 4). For a central ray with half-offset $h_0 = 500m$ and midpoint $x_0 = 2500m$ (red lines, lower part of Figure 3), the parameters K_1, K_2 and K_3 are calculated by forward modeling. Then, associated to this central ray in the upper part of Figure 3, the red curves represent the CRS operator obtained by expression (1).

The FO CRS stacking operator defined by formula (1) allows to simulate CO sections from multi-coverage data. As illustrated in Figure 3, for each sampling point $P_0(x_0, h_0, t_0)$ in the FO section to be

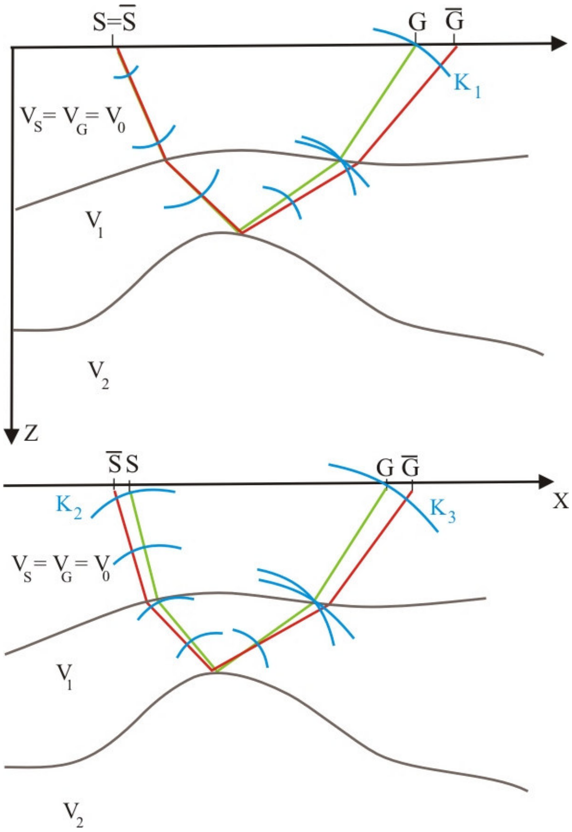

Figure 2: 2-D model of three homogeneous layers separated by curved and smooth interfaces: (a) Propagation of the wavefront of the CS experiment at different instants of time, (b) Propagation of hypothetical wavefronts of a CMP experiment at different instants of time.

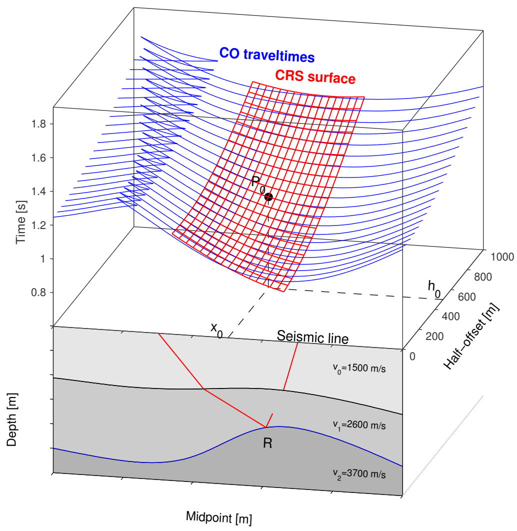

Figure 3: Lower part (front): 2D media with three homogeneous layers separated by homogeneous smooth interfaces and a finite-offset central ray, where x_0 is the midpoint, h_0 is the half-offset. Upper part: CO traveltime curves (blue color) related to primary reflections of the second interface, having the CRS stacking operator (red color) associated to point P_0.

simulated there exists a stacking surface defined by five parameters. The events contained in this surface will be summed and the result is assigned to the given point P_0.

HYPERBOLIC TRAVELTIME APPROXIMATION ASSOCIATED TO DIFFRACTED CENTRAL RAY

The hyperbolic traveltime approximation (1) considers a reflected central ray and traveltimes of paraxial rays in the vicinity of this central ray, which are also considered as being primary reflections. To consider the central ray as a diffracted ray, a new interpretation in the propagation of the wavefronts associated to the CS and CMP experiments, previously described, must be done. When a point R in subsurface (Figures 2a,b) is considered as a diffraction point, the Huygens Principle states that this point becomes a new source of wavefronts as soon as an incidence of wavefronts had just occurred. Under this assumption, the interpretation of the wave associated to a real CS experiment is the following: the wave generated by a point source S (origin of the central ray) propagates downwards and is diffracted at the located point in R. This diffraction point generates a new wavefront that propagates upwards along its central ray, emerging at G. In the CMP experiment, the wavefront propagation does not differs from the previous situation, but it must be considered now that R is a diffraction point. Therefore, the wavefront curvature K_1 emerging in G must have the same curvature of wavefront K_3, also emerging in G. Using the condition of diffraction, $K_1 = K_3$ in formula (1), to obtain

$$\begin{aligned} t^2(\Delta x_m, \Delta h) = & \left[t_0 + (\frac{\sin\beta_G}{v_G} + \frac{\sin\beta_S}{v_S})\ \Delta x_m + +(\frac{\sin\beta_G}{v_G} - \frac{\sin\beta_S}{v_S})\ \Delta h\right]^2 \\ & + t_0 \left[K_3\ \frac{\cos^2\beta_G}{v_G} - K_2\ \frac{\cos^2\beta_G}{v_S}\right]\ \Delta x_m^2 \\ & + t_0 \left[K_3\ \frac{\cos^2\beta_G}{v_G} - K_2\ \frac{\cos^2\beta_G}{v_S}\right]\ \Delta h^2 \\ & + 2\ t_0 \left[K_3\ \frac{\cos^2\beta_G}{v_G} + K_2\ \frac{\cos^2\beta_G}{v_S}\right]\ \Delta x_m\ \Delta h \end{aligned} \tag{2}$$

Now the hyperbolic traveltime approximation (Equation 2) depends only on four parameters: K_2, K_3, β_S and β_G.

By using the formula (2) we construct the stacking surface (Figure 4). Due to the fact that this operator (2) is associated to a diffracted central ray, then is called common-diffraction-surface (CDS). To distinguish the last operator from the present one, we shall denote it as FO CDS operator.

SEISMIC CONFIGURATIONS

In this section we present particular cases of formulas (1) and (2) for the following classical seismic configurations.

CMP gather

For this case, the paraxial source $\overline{S}$ and receiver $\overline{G}$ are located symmetrically with respect to the corresponding points S and G, on the central ray. Considering that the midpoint is common to the central and paraxial ray, the CMP condition reads: $\Delta x_m = 0$. Substituting this condition into equation (1), to obtain the CMP configuration traveltime

$$t^2(\Delta h) = \left[t_0 + (\frac{\sin\beta_G}{v_G} - \frac{\sin\beta_S}{v_S})\ \Delta h\right]^2 + t_0 \left[K_3\ \frac{\cos^2\beta_G}{v_G} - K_2\ \frac{\cos^2\beta_S}{v_S}\right]\ \Delta h^2 \tag{3}$$

Substituting this same condition in the general equation (2) for a diffraction point, we get the same expression (3).

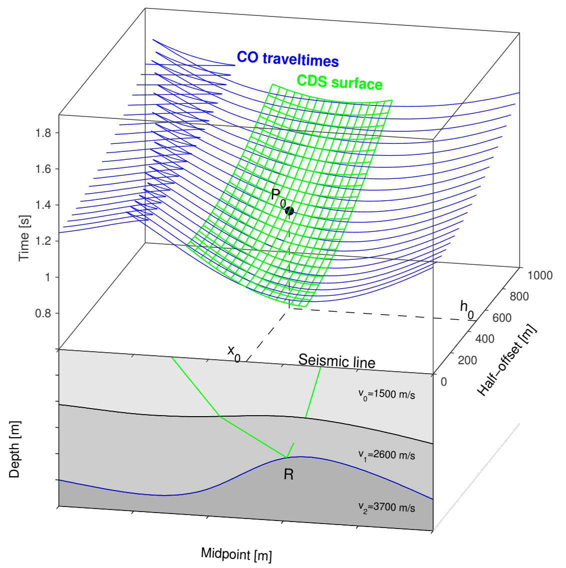

Figure 4: Lower part (front): 2D media with three homogeneous layers separated by curved and smooth interfaces and a FO central ray, where x_0 is the midpoint, h_0 is the half-offset. Upper part: CO traveltime curves (blue color) related to primary reflections of the second interface with the CDS operator (green color), associate to P_0.

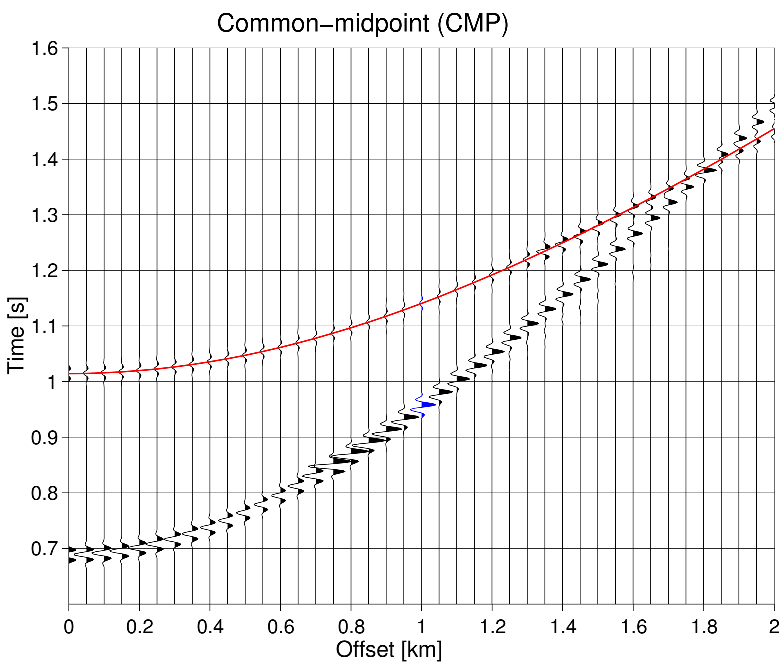

Figure 5: CMP section corresponding for the midpoint 2250 m. The red line corresponds to the traveltime calculated with equation (3) for the second reflector. For this configuration, the traveltime curve is the same for reflection and diffraction events.

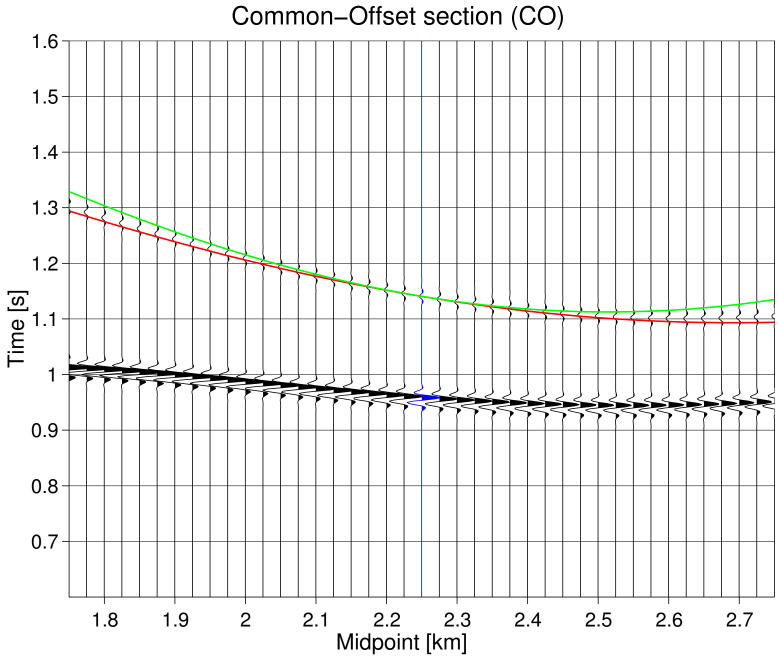

Figure 6: CO section which offset is 1 km. The red line corresponds to the traveltimes calculated with equation (4) and the green line corresponds to the traveltime calculated with equation (5).

Common-Offset (CO) gather

In this configuration, the paraxial source $\overline{S}$ and receiver $\overline{G}$ are shifted by the same amount and the same direction with respect to the corresponding points S and G, on the central ray. The CO condition reads: $\Delta h = 0$. This means that the sources-receiver pairs of the paraxial and central rays have the same half-offset.

The substitution of the CO condition into equation (1) gives

$$t^2(\Delta x_m) = \left[t_0 + (\frac{\sin\beta_G}{v_G} + \frac{\sin\beta_S}{v_S})\ \Delta x_m\right]^2 + t_0 \left[(4\ K_1 - 3\ K_3)\ \frac{\cos^2\beta_G}{v_G} - K_2\ \frac{\cos^2\beta_S}{v_S}\right]\ \Delta x_m^2 \tag{4}$$

Substituting in equation (2) the CO condition, it reads:

$$t^2(\Delta x_m) = \left[t_0 + (\frac{\sin\beta_G}{v_G} + \frac{\sin\beta_S}{v_S})\ \Delta x_m\right]^2 + t_0 \left[K_3\ \frac{\cos^2\beta_G}{v_G} - K_2\ \frac{\cos^2\beta_S}{v_S}\right]\ \Delta x_m^2 \tag{5}$$

In Figure 6 the offset of the CO section is 1.0 km. The traveltimes calculated by expressions (4) and (5) are represented by the red and green lines, respectively.

Common-Shot (CS) gather

For this configuration, the paraxial source always coincides with the source of the central ray. The CS condition reads: $\Delta x_m = \Delta h$. The substitution of this condition into equation (1)

$$t^2(\Delta h) = \left[t_0 + 2\ \frac{\sin\beta_G}{v_G}\ \Delta h\right]^2 + 4\ t_0 \left[K_1\ \frac{\cos^2\beta_G}{v_G}\right]\ \Delta h^2 \tag{6}$$

Applying the CS condition into equation (2), it reads:

$$t^2(\Delta h) = \left[t_0 + 2\ \frac{\sin\beta_G}{v_G}\ \Delta h\right]^2 + 4\ t_0 \left[K_3\ \frac{\cos^2\beta_G}{v_G}\right]\ \Delta h^2 \tag{7}$$

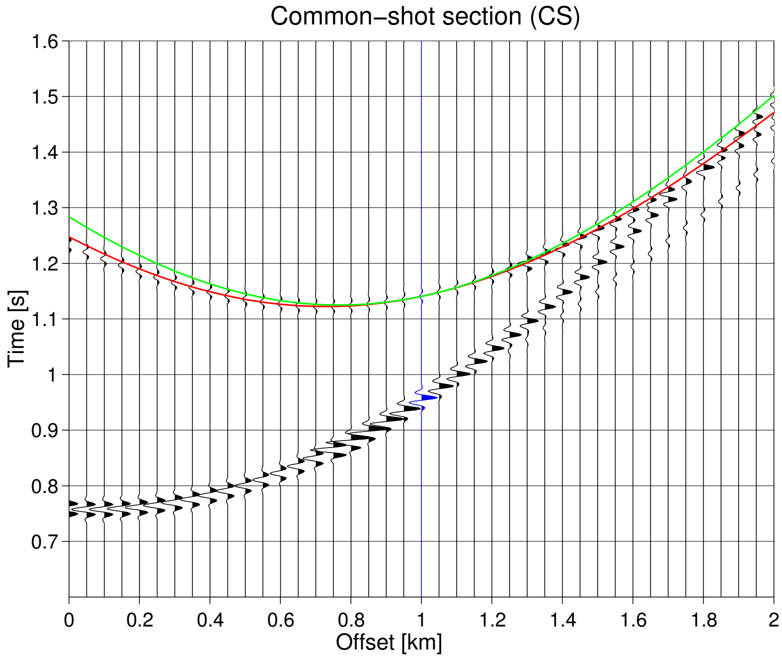

Figure 7: CS section: The red line corresponds to the traveltime calculated with equation (6) and the green line corresponds to the traveltime calculated with equation (7).

In Figure 7 it is shown a CS section where the position of the source is 1.75 km. The minimum offset is 0.0m and maximum offset is 2.0 km. The offset of the central ray is 1.0 km. The positions of the source and receiver of this central ray are 1.75 and 2.75 km, respectively.

Common-receiver (CR) gather

For this gather, the paraxial receiver always coincides with the receiver of the central ray. The CR condition reads: $\Delta x_m = -\Delta h$. The substitution of this condition into equation (1) gives

$$t^2(\Delta h) = \left[t_0 - 2\,\frac{\sin\beta_S}{v_S}\,\Delta h\right]^2 + 4\,t_0\left[K_1\,\frac{\cos^2\beta_G}{v_G} - K_2\,\frac{\cos^2\beta_S}{v_S} - K_3\,\frac{\cos^2\beta_G}{v_G}\right]\,\Delta h^2\;. \qquad (8)$$

By considering this condition for a diffracted central ray into equation (2), we obtain

$$t^2(\Delta h) = \left[t_0 - 2\,(\frac{\sin\beta_S}{v_S}\,\Delta h\right]^2 - 4\,t_0\left[K_2\,\frac{\cos^2\beta_S}{v_S}\right]\,\Delta h^2 \qquad (9)$$

In Figure 8 is shown the CR section. The fixed receiver is located at 2.75 km. The first source is located at 0.75 km, and the rest of the sources are located for both sides of the first source. The traveltimes calculated by expressions (8) e (9) are represented by red and green lines, respectively.

SENSIBILITY ANALYSIS OF THE FO CRS STACKING OPERATOR

To define the priority in the parameters search, is necessary investigate the sensibility of the FO CRS stacking operator with respect to the kinematic data-derived attributes. By analyzing the first derivative of the FO CRS traveltimes with respect to each one of the searched-for parameters and perturbing each parameter, we describe the behavior of the FO CRS stacking surface.

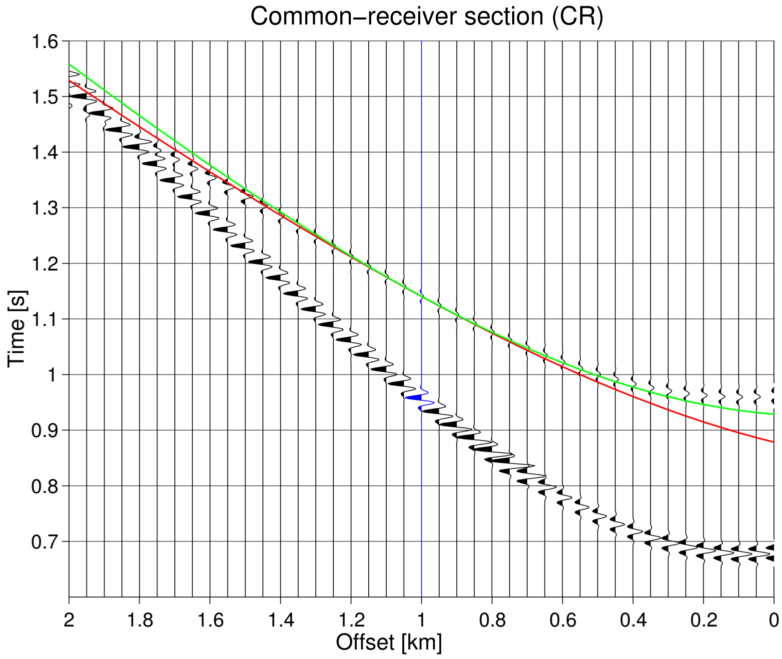

Figure 8: CR section. The red line corresponds to the traveltimes calculated with equation (8) and green lines correspond the traveltimes calculated with equation (9).

First derivative analysis of the wavefront attributes

The first derivative of the FO CRS operator with respect to the parameters to let us to analyze the sensibility of this approximation. The derivatives were done by using the FO CRS and CDS CRS stacking operators with respect the attributes:$\beta_S, \beta_G, K_1, K_2, K_3$.

These derivatives, are shown in the Figures 10 and 9. We remind that in this analysis we considered a fixed point P_0. We use different half-offsets, as instance $h = 0.0km,\ h = 0.25km,\ h = 0.5km,\ h = 0.75km,\ h = 1.0km$. To difference the curves of these derivatives, we use different colors: blue for $h = 0.0km$, magenta for $h = 0.25km$, cyan for $h = 0.5km$, green for $h = 0.75km$ and red for $h = 1km$.

In Figure 10, we observe in the vicinity of the central ray x_0, the traveltime derivatives with respect parameters K_2 and K_3 are sensitives with respect Δx_m and Δh, while that the parameter K_1 is less sensitive to the changes of Δx_m and Δh. In Figure 9 for variations along the coordinates Δx_m and Δh, shows the derivatives higher sensitives with respect the parameters β_S and β_G.

For the central point analyzed the traveltime function is very sensitive to the β_S and β_G, followed of the parameters K_3 and K_2. This is an indicator that the parameters can be very well determined by search processes (optimization). In the case of the parameters K_2 and K_3, this operator shows a higher degree of difficulty to determinate them. For the parameter K_1, the FO CRS traveltime showed less sensibility. In this case, this parameter will be determined with difficulty and minor precision.

CO-CRS STACKING STRATEGY

For the simulation of CO sections with the CO-CRS stacking method, is needed to determine five parameters $\beta_S, \beta_G, K_1, K_2, K_3$ or wavefront attributes from multicoverage data. Here, we use the FO CRS operator associated to a certain sampling point P_0 in the CO section to determine from multicoverage data these parameters.

The crucial part of this procedure is the determination of the stacking operator from seismic data to the optimization process using as an objective function the coherence (semblance) section. In this work, in-

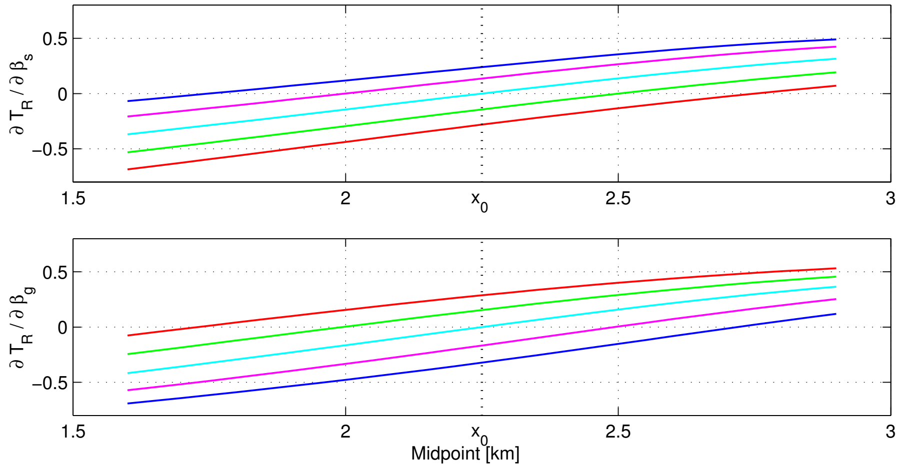

Figure 9: Sensibility through FO CRS traveltime derivative with respect B_S (top) and B_G (middle) and K_3 (bottom) for different offsets, $h = 0.0km(bluecurve), \ h = 0.25km(magentacurve), \ h = 0.5km(cyancurve), \ h = 0.75km(greencurve)$ and $h = 1.0km$ (red curve).

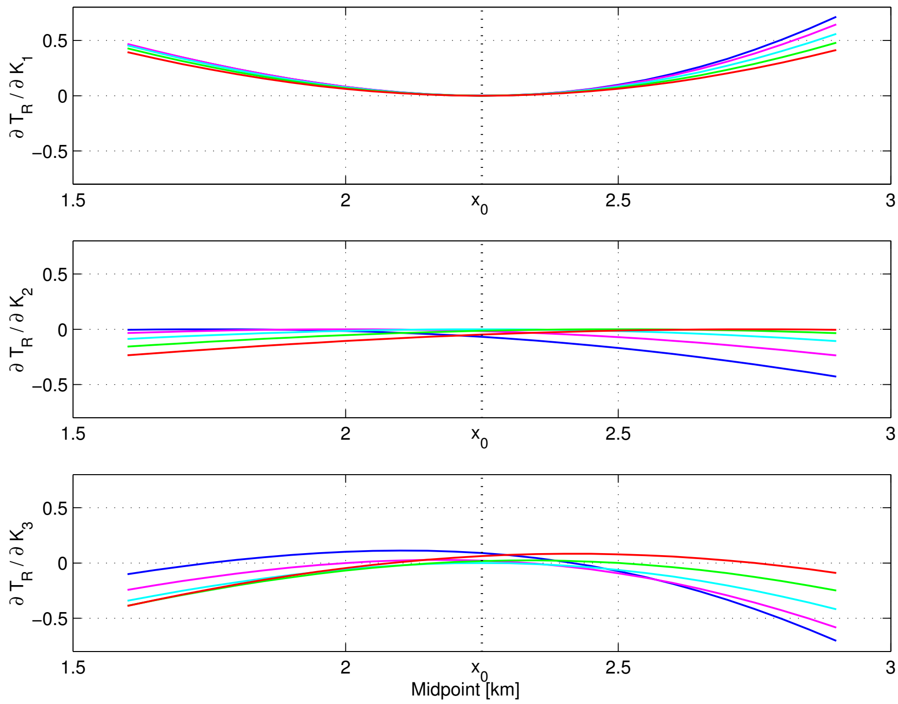

Figure 10: Sensibility through FO CRS traveltime derivative with respect K_1 (top), K_2 (middle) and K_3 (bottom) for different offsets, $h = 0.0km$ (blue curve), $h = 0.25km$ (magenta curve), $h = 0.5km$ (cyan curve), $h = 0.75km$ (green curve) and $h = 1.0km$ (red curve).

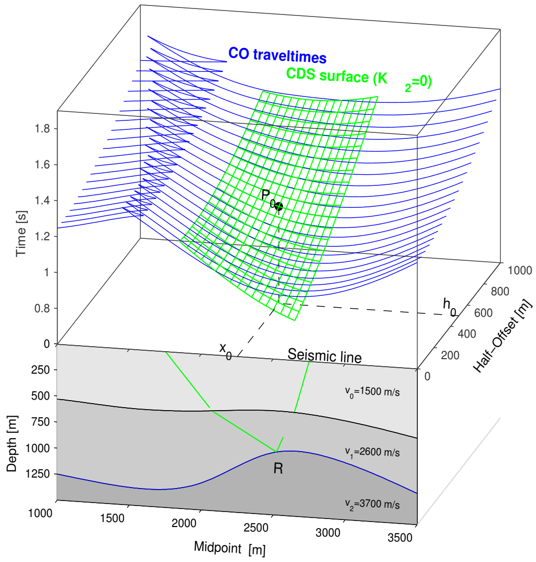

Figure 11: Lower part (front): 2D media with three homogeneous layers separated by curved and smooth interfaces and a FO central ray, where x_0 is the midpoint, h_0 is the half-offset. Upper part: CO traveltime curves (blue color) related to primary reflections of the second interface with the CDS operator when $K_2 = 0$ (green color), associate to P_0.

stead of using CMP, CO and CS sections to determine the stacking parameters (Zhang et al., 2001), they are determined using operators or stacking surfaces defined in the domain $(\Delta x_m, \Delta h)$, which are defined by three, four and five parameters. Now, we consider the CO-CRS algorithm proposed below, where the $VeryFastSimulatedAnnealing(VFSA)$ global optimization algorithm for the initial determination of these parameters is applied. To refine these parameters, we use the $Quasi - Newton(QN)$ local optimization algorithm. This strategy is summarized in Figure 12

First step: Three-dimensional search (β_S,β_G,K_1)

From multicoverage data, using the $VFSA$ algorithm, three parameters (β_S,β_G,K_1) are determined by applying a tri-dimensional search. To obtain and to use the stacking operator defined by three parameters, it is introduced the condition $K_2 = 0$ (Figure 11) into equation (2). This condition is applied due to the fact of that CO-CRS stacking operator has not shown sensitivity for an sample interval of variation of this parameter.

Second step: Uni-dimensional search (K_2)

Using the parameters determined in the previous step from multicoverage data, also using the VFSA global optimization algorithm, the parameter K_2 is determined for each sampling point of the CO section. In this step, we use the stacking operator defined by equation (2).

Third step: Uni-dimensional search (K_3)

Using the four parameters determined in the previous step from multicoverage data and using the $VFSA$ global optimization algorithm, the parameter K_3 is determined for each sampling point of the CO section. In this step, the stacking operator is defined by equation (1).

Fourth step: Refinement of the five parameters (β_S,β_G,K_1,K_2,K_3)

To determine the best values of the five parameters simultaneously (β_S,β_G,K_1,K_2,K_3) and consequently, the best CO-CRS stacking operator, the QN local optimization algorithm is applied. As an initial approximation for the local search in the multicoverage data, the five resulting parameters of the two previous steps are used. In this step, the objective function (semblance) uses the general formula (1) to obtain the FO CRS stacking operators in the optimization process. The five parameters derived in this step are used to simulate the final CO section.

CONCLUSIONS AND PERSPECTIVES

From the traveltime formula of reflected paraxial rays in the vicinity of a central ray with finite-offset, it was derived a particular traveltime formula for paraxial rays in the vicinity of a central ray associated to a diffraction point in depth. This new approximation depends on four parameters, thus reducing the original formula in one parameter. Also the stacking operators (equations 1 and 2) have been compared, where it was verified that this new formula (equation 2) defines a new operator that can be used to simulate CO sections by means of the CRS stacking technique. Comparisons of reflections and diffractions traveltimes have also been made, following the main seismic configurations (CMP, CR, CS and CO), where it was also verified that the paraxial rays traveltimes associated to a diffracted central ray have a good fitting with respect to the reflected events. This operator (equation 2) is an alternative to simulate CO sections. In this work it is shown that the traveltime formulas associated to a diffraction point in depth can also be used to identify and extract diffractions, where it can be used the CO, CS and CR configurations. Finally, we propose a new strategy to estimate the five parameters in the FO CRS stacking method. The first third steps use the SA global optimization method. The fourth step uses the QN local optimization algorithm.

ACKNOWLEDGMENTS

This work was kindly supported by the sponsors of the *Wave Inversion Technology (WIT) Consortium*, Karlsruhe, Germany.

REFERENCES

Bergler, S., Duveneck, E., Höcht, G., Zhang, Y., and Hubral, P. (2001a). Common-Reflection-Surface stack for common-offset: practical aspects. *63rd Annual Internat. Mtg., Soc. Expl. Geophys., Expanded Abstracts*, page P076.

Bergler, S., Duveneck, E., Höcht, G., Zhang, Y., and Hubral, P. (2001b). Common-Reflection-Surface stack for converted waves. *Wave Inversion Technology (WIT) Report (Germany)*, pages 24–31.

Bergler, S., Mann, J., and Höcht, G.and Hubral, P. (2002). The Finite-Offset CRS stack: an alternative stacking tool for subsalt imaging. *72nd Annual Internat. Mtg., Soc. Expl. Geophys., Expanded Abstracts*.

Bergler, S., Zhang, Y., Chira, P., Vieth, K.-U., and Hubral, P. (2001c). Common-Reflection-Surface stack and attributes. *7th International Congress of the SBGf, BRAZIL. Oral session WS1-Workshop Seismic Imaging*.

Boelsen, T. (2004). 2D CO CRS stack for top-surface topography. *Wave Inversion Technology (WIT) Report (Germany)*, pages 63–76.

Boelsen, T. and Mann, J. (2004). 2D CO CRS stack for ocean bottom seismics and multi-component data. *Wave Inversion Technology (WIT) Report (Germany)*, pages 77–88.

Boelsen, T. and Mann, J. (2005a). 2D CO CRS stack for OBS and VSP data and arbitrary top-surface topography. *EAGE 67th Conference and Technical Exhibition*, page P181.

Boelsen, T. and Mann, J. (2005b). Common-Reflection-Surface stack for OBS and VSP geometries and multi-component seismic reflection data. *9th International Congress of the Brasilian Geophysical Society*.

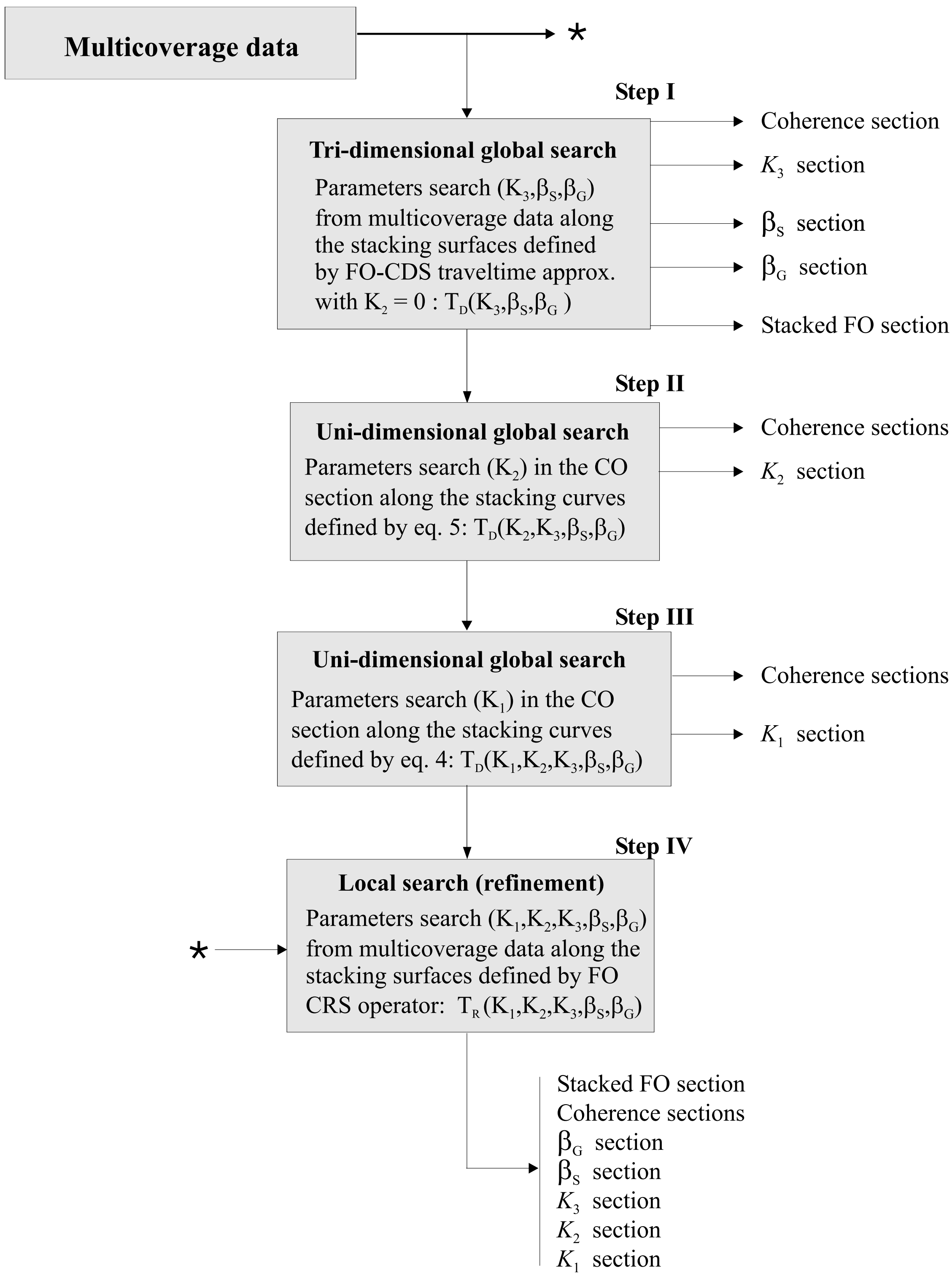

Figure 12: Flowchart of the CO-CRS stacking algorithm.

Bortfeld, R. (1989). Geometrical ray theory: Rays and traveltimes in seismic systems (second order approximation of the traveltimes). *Geophysics*, 1:342–349.

Cerveny, V. and Psensik, I. (1988). SEIS88, Ray tracing program package. *Charles University, Prague (Czechoslovakia).*

Chira-Oliva, P., Cruz, J. C. R., Bergler, S., and Hubral, P. (2003). Sensibilty analysis of the FO CRS traveltime approximation. *8th International Congress of the SBGf, BRAZIL.*

De Bazelaire, E. (1988). Normal moveout revisited inhomogeneous media and curved interfaces. *Geophysics*, 53(2):143–157.

Garabito, G., Cruz, J. C. R., Hubral, P., and Costa, J. (2001). Common reflection surface stack by global optimization. *71th Annual Internat. Mtg., Soc. Expl. Geophys, USA*.

Gelchinsky, B., Berkovitch, A., and Keydar, S. (1999a). Multifocussing homeomorphic imaging Part 1. Basic concepts and formulas. *J. Appl. Geoph.: Special Issue: Macro-Model Independent Seismic Reflection Imaging*, 42(3,4):229–242.

Gelchinsky, B., Berkovitch, A., and Keydar, S. (1999b). Multifocussing homeomorphic imaging Part 2. Multifold data set and multifocusing. *J. Appl. Geoph.: Macro-Model Independent Seismic Reflection Imaging*, 42(3,4):243–260.

Gelchinsky, B. and Keydar, S. (1999). Homeomorphic imaging approach - theory and practice. *J. Appl. Geoph.*, 42(3,4):169–228.

Hubral, P. and Krey, T. (1980). Interval velocities from seismic reflection traveltime measurements. *Society of Exploration Geophysicists, Tulsa, OK,203 p.*

Jäger, R., Mann, J., Höcht, G., and Hubral, P. (2001). Common Reflection Surface Stack: Image and Attributes. *Geophysics*, 66:97–109.

Landa, E., Gurevich, B., Keydar, S., and Trachtman, P. (1999). Application of multifocusing method for subsurface imaging. *J. Appl. Geophys.*, 3:283–300.

Müller, T. (1999). The common reflection surface stack method - seismic imaging without explicit knowledge of the velocity model. *Ph.D. Thesis, University of Karlsruhe, Germany*.

Zhang, Y., Bergler, S., and Hubral, P. (2002). Model-independent Travel-time Attributes for 2-D, Finite-offset Multicoverage Reflections. *Pure and Applied Geophys.*, 159:1–16.

Zhang, Y., Bergler, S., Tygel, M., and Hubral, P. (2001). Common-Reflection-Surface (CRS) stack for common-offset. *Geophys.Prosp.*, 49:709–718.